6D.1 THE EVOLUTION OF RAINFALL AND CONVECTION IN RAPIDLY INTENSIFYING TROPICAL CYCLONES BASED ON 16 YEARS OF TRMM DATA

Cheng Tao* and Haiyan Jiang
Department of Earth & Environment, Florida International University, Miami, FL

1. INTRODUCTION

Rainfall and convection within the inner core region of TCs have been linked with RI in several satellite-based observational studies (e.g., Jiang 2012; Tao and Jiang, 2015). Composites and statistical analysis of these studies are very useful in distinguishing the inner-core rainfall and convection distributions of RI storms from those in other intensity change categories. But there are some limitations as well. Examining RI only in terms of future 24-h intensity change cannot fully address the role of convection in RI, because of the absence of temporal information before the RI onset, at the beginning of RI, during the middle of RI, and within the ending period of RI. Convective evolution in RI storms is examined extensively in recent case studies (e.g., Stevenson et al. 2014). However, all the mechanisms that proposed triggering the RI by case studies need to be statistically quantified based on a larger dataset.

2. DATA AND METHODOLOGY

The best track data are used to determine RI events from a total of 1518 TCs between 1998 and 2013. Here, an RI event is defined as multiple, continuous, and overlapping 24-h periods where the maximum sustained winds of each period increased by at least 30 kt (Fig. 1). The dataset for this study is derived from the TRMM Tropical Cyclone Precipitation Feature (TCPF) database (Jiang et al. 2011). The storm center interpolated with best track information is manually adjusted to better align with the imageries of PR and TMI 37 GHz channel (Zagrodnik and Jiang 2014).

Fig. 1. Definition of an RI event using the best track data. Here, Vmax and Vmax+24 represent the maximum sustained wind at the current synoptic time and 24 hours in future, respectively.

**Corresponding author address:* Cheng Tao, Dept. of Earth & Environment, Florida International University, 11200 SW 8th St, Miami, FL 33199.
Email: ctao003@fiu.edu

Several criteria have been applied to the selection of overpasses viewed by the TRMM TMI. Firstly, the interpolated storm center must be over water at the current observational time and 24 hours in the future. Secondly, overpasses must capture the innermost 200 km area. Thirdly, the storm intensity must be between tropical storm and category 2 hurricane. Fourthly, storms under unfavorable environment are excluded. According to the TRMM observational time and the start/end time of RI events, the selected TMI overpasses are classified into 14 categories (Table 1).

Based on the 85 GHz polarized corrected temperature (PCT), four types of precipitation-convection are defined: very deep convection (PCT85 ≤ 160K), moderately deep convection (160K < PCT85 ≤ 200K), moderate precipitation (200K < PCT85 ≤ 260K), and shallow precipitation (260K < PCT85 ≤ 275K). For identified TMI pixels within the innermost 250 km, the scatterplot of their real colors in the 37 GHz color composite products (Lee et al. 2002) is displayed and three regions (pink, dark cyan, and bright cyan) are identified.

Table 1. Number of selected TRMM TMI overpasses before RI, during RI, and in the RI ending period.

Category		All	RI	SI	N	W
Before RI	36~48 h before	26	0	14	10	2
	24~36 h before	39	0	25	14	0
	18~24 h before	32	0	21	11	0
	12~18 h before	47	0	37	10	0
	6~12 h before	44	0	42	2	0
	0~6 h before	36	0	36	0	0
During RI	0~6 h after	41	41	0	0	0
	6~12 h after	45	45	0	0	0
	12~18 h after	45	45	0	0	0
	18~54 h after	61	61	0	0	0
RI ending	18~24 h before	44	0	43	1	0
	12~18 h before	55	0	52	2	1
	6~12 h before	44	0	23	18	3
	0~6 h before	36	0	13	18	5
All		595	192	306	86	11

3. RESULTS

a. Evolution of rainfall and convection distribution

Both the percentages of pixels with rain rate > 0.5 (Fig. 2a) and 1 mm/hr (Fig. 2b) increase significantly around 3-9 hours before RI onset and continue to increase after RI begins. The percent occurrence of rain rate > 5 (Fig. 2c) and 10 mm/hr

(Fig. 2d) steadily increase with time approaching the RI onset while rapidly increase around 3-9 hours after RI onset.

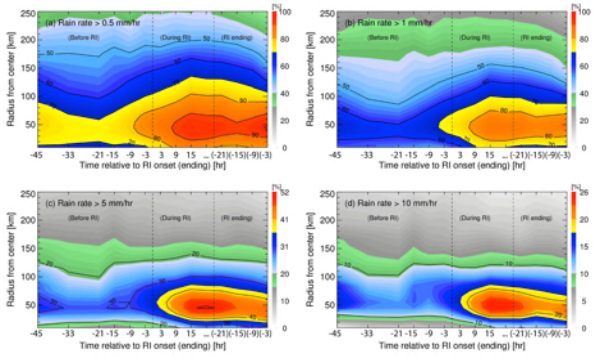

Fig. 2. Hovmöller diagrams of azimuthally averaged percent occurrence of rain rate (a) > 0.5 mm/hr, (b) > 1 mm/hr, (c) > 5 mm/hr, and (d) > 10 mm/hr. The averages are shown from the storm center out to 250 km. Dashed lines from left to right represent the RI onset and 24 hours before RI ends.

Very deep convection peaks about 15 hours before RI onset and rapidly decreases in the following 24 hours (Fig. 3a). The areal coverage of very deep convection does not reach 1% during RI until in the end of RI event. The areal coverage of moderate precipitation significantly increases when storms begin to RI and this increase continues at a higher rate as RI continues (Fig. 3c). Shallow precipitation is most frequent between three hours before RI onset and nine hours after (Fig. 3d). The percent occurrence of pink in 37 GHz color composites increases significantly at about nine hours after RI begins (Fig. 4a). Bright cyan first decreases and then increases at about nine hours prior to the onset of RI (Fig. 4b). Generally, > 30% of the innermost 50 km area is covered by dark cyan during the whole period of analysis (Fig. 4c).

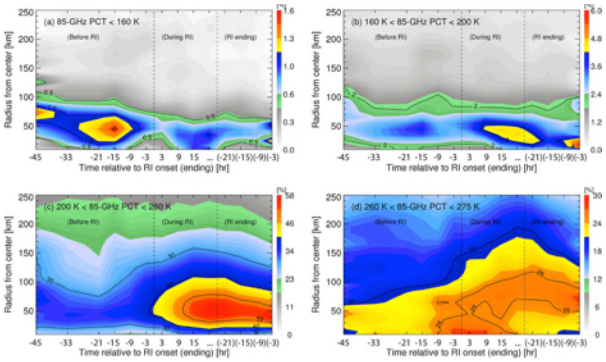

Fig. 3. As in Fig. 2, but for percent occurrence of 85 GHz PCT (a) < 160 K, (b) 160-200 K, (c) 200-260 K, and (d) 260-275 K.

Results above show that RI onset follows an increased areal coverage of rainfall with light-to-moderate raining rate and shallow precipitation around the storm center. The shear-relative composites further indicates that this increase is first observed in the upshear-left (UL) quadrant 0-12 hours before RI onset and then rotates cyclonically as RI continues, concentrating upshear-right (UR) for RI initial storms while right of the shear vector during RI continuing.

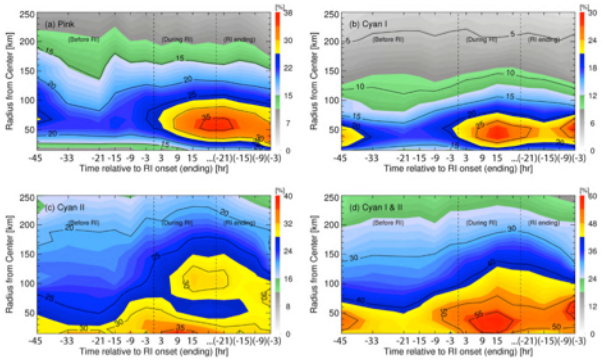

Fig. 4. As in Fig. 2, but for percent occurrence of (a) pink, (b) bright cyan, (c) dark cyan, and (d) bright+dark cyan.

b. Evolution of vortex vertical alignment

The Automated Rotational Center Hurricane Eye Retrieval (ARCHER) product (Wimmers and Velden 2010) is applied to determine the rotational center in TMI 37 and 85 GHz imageries. The vortex misalignment refers to the difference between the rotational centers of 37 and 85 GHz imageries.

The magnitude of vortex vertical misalignment (Fig. 5) does not decrease much until in the middle of RI (i.e., RI continuing), suggesting that vertical alignment is a result or positive feedback rather than the trigger of RI. The distributions of the vortex vertical misalignment are also analyzed according to the direction of vertical wind shear. Generally, direction of the displacement of 85 GHz rotational centers concentrate in the downshear-left quadrant (DL). But differences exist among various RI event-based categories. The tilt of vortex is much more DL-dominated for storms before the RI onset while more evenly distributed in both DL and downshear-right (DR) quadrants for those after RI begins.

4. CONCLUSION

The onset of RI is closely associated with an increased coverage of rainfall and shallow precipitation. A statistically significant increase in the percent occurrence of rain rate > 0.5 and 1 mm/hr, shallow precipitation, and cyan regions is

noted 0-12 hours prior to RI onset, which in turn could be used as potential parameters to forecast the onset of RI. The tilt of vortex is large near the onset of RI and decreases rapidly in the middle of RI events.

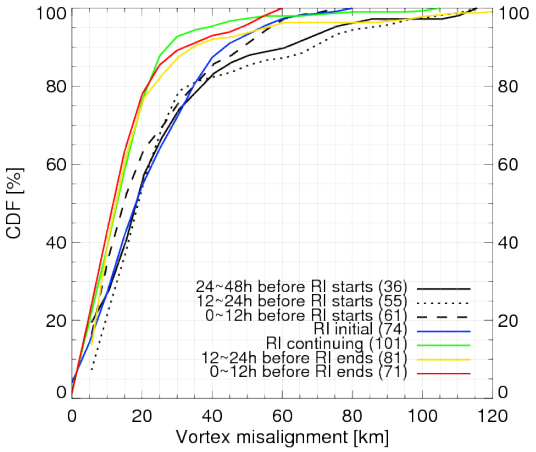

Fig. 5. Cumulative distribution functions (CDFs) of vortex misalignment for each RI event-based category. Number in parenthesis indices the sample size.

REFERENCES

Jiang, H., 2012: The relationship between tropical cyclone intensity change and the strength of inner-core convection. *Mon. Wea. Rev.,* 140, 1164–1176.

Jiang, H., C. Liu, and E. J. Zipser, 2011: A TRMM-based tropical cyclone cloud and precipitation feature database. *J. Appl. Meteor. Climatol.,* 50, 1255-1274.

Lee, T. F., F. J. Turk, J. Hawkins, and K. Richardson, 2002: Interpretation of TRMM TMI images of tropical cyclones. *Earth Interact.,* 6, 1–17.

Stevenson, S. N., K. L. Corbosiero, and J. Molinari, 2014: The convective evolution and rapid intensification of Hurricane Earl (2010). *Mon. Wea. Rev.,* 142, 4364–4380.

Tao, C., and H. Jiang, 2015: Distributions of shallow to very deep precipitation–convection in rapidly intensifying tropical cyclones. *J. Climate,* 28, 8791–8824.

Wimmers, A., and C. Velden, 2010: Objectively Determining the Rotational Center of Tropical Cyclones in Passive Microwave Satellite Imagery. *J. Appl. Meteor. Climatol.,* 49, 2013–2034.

Zagrodnik, J. P., and H. Jiang, 2014: Rainfall, convection, and latent heating distributions in rapidly intensifying tropical cyclones. *J. Atmos. Sci.,* 71, 2789-2809.